





Vine-Like, Power Soft Gripper Based on Euler's Belt Theory

Hiroto Kodama , Tohru Ide , Feng Yunhao , Hiroyuki Nabae , *Member, IEEE*, and Koichi Suzumori 

Abstract—Soft robots hold the potential for use in disaster sites where it is difficult to predict the external environment and the manipulation of irregularly shaped heavy objects is required. However, existing soft robots possess the low load capacity. Therefore, we propose a vine-like, power soft gripper that grasps an object by wrapping it, and we fabricated a prototype. The gripper is based on Euler's belt theory, the load capacity increases with the wrap angle and it is demonstrated by load capacity measurements. A grasping experiment demonstrated that the gripper could grasp objects of various shapes. This gripper wraps around an object using the restoring force exerted by the constant-force spring. Hence, the gripper cannot lift heavy objects that tend to rotate during lifting. However, it was confirmed that a twin-gripper with opposite helical directions could grasp such objects. It was also confirmed that twin-gripper could grasp an object weighing 1660 N although its two constant-force springs possess a small load of 43 N. This indicates that the grasping load force surpassed that generated by the spring coiling force. Finally, the gripper was attached to a construction machine robot, and a pick-and-place demonstration was conducted.

Index Terms—Power soft robot, soft gripper, vine gripper, pneumatic actuator, Euler's belt theory.

I. INTRODUCTION

VARIOUS soft grippers that focus on shape adaptability have been developed [1], [2]. Many grippers are inspired by biological organisms, and grippers composed of links and soft materials grasp objects like a human hand [3], [4], [5] have been developed. Unlike grippers that mimic human fingers, finger-type grippers that do not have links and are composed only of soft materials have also been developed [6], [7], [8], [9]. These grippers have an infinite number of degrees of freedom, which enable them to grasp objects in a manner that follows the object. Further, grippers that wrap around objects with twisting, similar to a plant vine [10], [11], have also been developed. Their helical motion can be adapted to more complex shapes. A bag-shaped gripper containing particles can be grasped by pressing it against an object and changing its hardness [12], [13]. The ability of the grippers to deform and conform to the

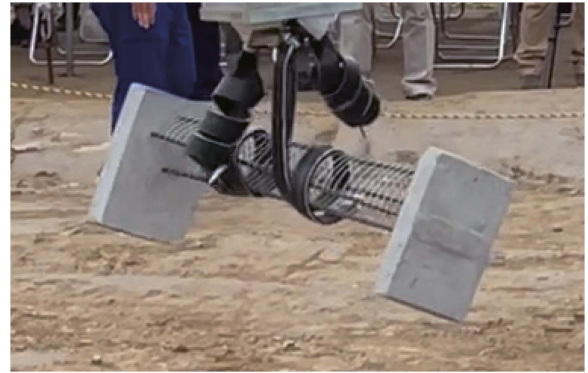


Fig. 1. Twin-gripper each with opposite helix directions grasps concrete block.

shape of an object provides high shape adaptability. Owing to this characteristic, grippers are anticipated to be utilized at disaster sites where the environment is constantly changing and the removal of irregularly shaped objects is required. However, the load capacity of a soft gripper is not sufficiently large to manage them.

Various soft grippers aimed at achieving the high load capacity have been developed. For instance, The load capacity can be increased by mimicking octopus suction cups [14], [15], [16] or gecko toes [17], [18], [19]. Among them, an elastomer actuator featuring a gecko-inspired adsorption structure on its surface [19] possesses a load capacity of 110 N. These grippers increase the load capacity by adsorption in addition to the grasping by wrapping. Grippers that expand inward to envelop and grasp an object can increase the load capacity by increasing the contact area [20], [21], [22]. Among them, the large enveloping gripper can rescue a child doll and can grasp an object of 539 N [22]. Furthermore, a gripper equipped with a locking mechanism that possesses a load capacity of approximately 1000 N per gripper was developed [23]. However, this gripper is susceptible to external disturbances and exhibits diminished shape adaptability compared to conventional soft grippers. In addition, these load capacities do not satisfy the requirements for grasping heavy objects such as fallen trees. The disaster-responding special-purpose machinery [24] can grasp approximately 400 N with two arms, and the robot that aimed at the rescue operation in the danger zone such as the stricken area etc. [25] can grasp approximately 10,000 N with two arms. Thus, further improvement in the load capacity is required. This facilitates a need to enhance the load capacity of soft grippers for use at sites, such as disaster sites. To realize high load capacity,

Manuscript received 1 September 2023; accepted 1 February 2024. Date of publication 13 February 2024; date of current version 21 February 2024. This letter was recommended for publication by Associate Editor C. Majidi and Editor C. Laschi upon evaluation of the reviewers' comments. This work was supported by JST [Moonshot R&D] under Grant JPMJPS2032. (Corresponding author: Hiroto Kodama.)

The authors are with the Department of Mechanical Engineering, Tokyo Institute of Technology, Tokyo 152-8550, Japan (e-mail: kodama.h.ad@m.titech.ac.jp).

This letter has supplementary downloadable material available at <https://doi.org/10.1109/LRA.2024.3365268>, provided by the authors.

Digital Object Identifier 10.1109/LRA.2024.3365268

we focused on a soft gripper that wraps around an object in a helical shape [26], [27], [28].

In this study, we proposed and fabricated a prototype of vine-like, power soft gripper that can grasp heavy objects by wrapping them in a manner similar to a vine, as shown in Fig. 1. The gripper primarily consists of a hose and a constant-force spring and wraps around objects by the restorative force of spring. Based on Euler's belt theory, the larger the angle at which it wraps around objects in a helical shape, the higher the load capacity than that generated by the coiling force of the spring itself owing to friction. Furthermore, it works stiffly and powerfully only in the tensile direction, resulting in high shape adaptability to objects. Single gripper cannot lift heavy objects that tend to rotate during lifting in proposed principle. However, such objects can be grasped using a twin-gripper in the opposite helix directions, as shown in Fig. 1. Finally, we plan to realize a gripper that can be used at disaster sites where high shape adaptability and the high load capacity are required.

The contribution of this work is providing design method of the soft gripper with high load capacity using friction. Additionally, the prototype of gripper demonstrated its usefulness.

The remainder of this paper is organized as follows. Section II proposes vine-like, power soft gripper. Section III extends Euler's belt theory and describes the modeling of the gripper load capacity. Section IV describes the prototype. Section V describes the grasping experiment using one gripper, a twin-gripper to measure the load capacity of the gripper with the wrap angle, verifies the adaptability of the gripper shape and a pick-and-place demonstration using the gripper attached to a construction machine robot. Finally, Section VI presents the conclusions and future work.

II. STRUCTURE AND WORKING PRINCIPLE

Euler's belt theory considers a situation wherein a belt is wrapped around a cylindrical bar that does not rotate. When a force is applied to one side of the belt, the force required to pull the other side and slide the belt increases exponentially according to the wrap angle. In this paper, the wrap angle is defined as the angle of rotation of the helix. From this theory, it can be shown that the tension immediately before the onset of belt slippage increases exponentially with the wrap angle. Therefore, the load capacity of the gripper, that grasps an object by coiling, is expected to increase according to the wrap angle. To realize wrapping motion, we propose vine-like, power soft gripper with the structure shown in Fig. 2. The gripper primarily consists of a hose and a constant-force spring, which is a spiral spring with a constant force required to pull it out. As shown in Fig. 2(a), a constant-force spring is inserted into the hose, which is initially wound into a helical shape. Therefore, when air pressure is applied, the gripper extends from the base, as shown in Fig. 2(b), and in a straight line, as shown in Fig. 2(c). Subsequently, the gripper is rolled back from the tip by depressurizing the air pressure to atmospheric pressure, as shown in Fig. 2(b), and it returns to the initial state, as shown in Fig. 2(a). When grasping an object, the gripper is first approached with the applied air pressure. If the object is light, the tip of the gripper

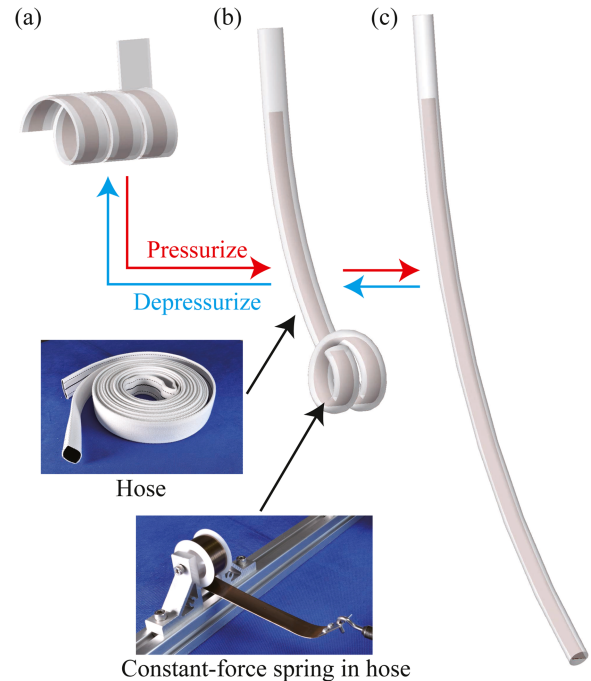


Fig. 2. Structure of vine gripper.

hooks onto the object, and the gripper wraps around the object while pulling the object toward itself. If the object is heavy, the gripper wraps around the object while the gripper tip slips on the object.

Many pneumatically or hydraulically operated vine-shaped soft grippers [26], [27], [28] grasp objects under pressure. Therefore, it is considered that the gripper may rupture due to stress concentration while grasping an object. Furthermore, if the gripper is damaged, a continuous supply of energy is required, and the object may fall due to insufficient pressure. Vine-shaped grippers made of shape memory polymer [10] must be heated when grasping an object, and energy must be supplied to the gripper while grasping the object. However, because the proposed gripper grasps an object by depressurizing it, the gripper does not rupture due to stress concentration while grasping the object, and the object is not considered to fall even if the gripper surface is damaged. Additionally, the gripper only applies air pressure when approaching an object and does not require an energy supply to maintain the object in its grasp. Thus, the gripper can maintain a grasp even if the energy source is a problem. Consequently, it is considered that the safety of maintaining the grasped state can be secured compared to the conventional soft gripper.

III. MODELING OF LOAD CAPACITY

The proposed gripper grasps an object by wrapping it. When lifting an object, the gripper exerts it with a force that rotates it around the axis of rotation of the helix drawn by the gripper as shown in Fig. 3. Therefore, if the object's center of gravity is close to the gripper's axis of rotation, it can undergo a rotational movement as shown in Fig. 3(a). The gripper wraps around the

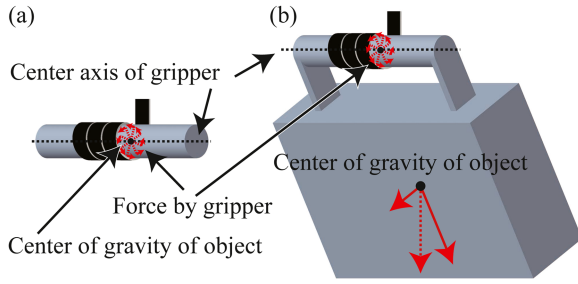


Fig. 3. Rotation of the object. (a) Center of gravity of an object is close to center axis of gripper. (b) Center of gravity of an object is far from center axis of gripper.

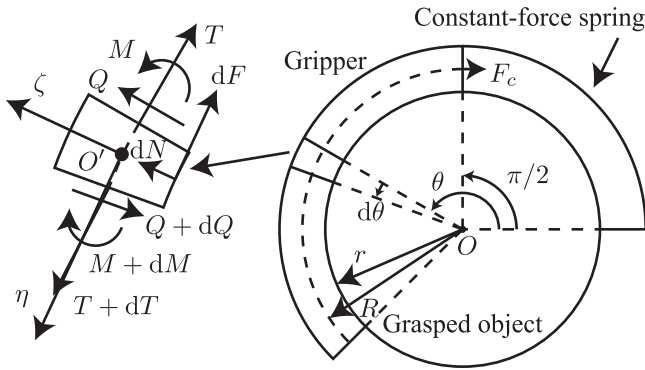


Fig. 4. Force acting on infinitesimal section when this gripper is wrapped around non-rotating cylindrical rod.

object due to the restoring force of the constant-force spring, because a constant-force spring is inserted inside the gripper. A constant-force spring is a spiral spring that is affixed to a rotating shaft designed to extend under a consistent pullout force. Therefore, if the object rotates during lifting, the gripper cannot lift an object that weighs more than the load of the constant-force spring.

When the object's center of gravity is farther from the gripper's axis of rotation, the moment caused by gravity acting on the object increases during its rotation, and the rotation stops as shown in Fig. 3(b). Therefore, in this case, based on Euler's belt theory, the load capacity, which is the load immediately before the gripper begins to slip, can be increased with the wrap angle. Euler's belt theory assumes that the thickness of the belt is significantly smaller than the diameter of the cylindrical bar. Therefore, this theory can be extended by considering belt thickness. Because this gripper wraps around an object owing to the restoring force of the constant-force spring, the belt can be regarded as a curved beam.

Fig. 4 shows the force applied to a minute portion of the gripper when wrapped around a non-rotating cylindrical bar. Considering the equilibrium of the forces and moments in the η and ζ directions in this infinitesimal section, the following holds for each:

$$(Q(\theta) + dQ(\theta)) \cos \frac{d\theta}{2} - Q(\theta) \cos \frac{d\theta}{2}$$

$$+ (T(\theta) + dT(\theta)) \sin \frac{d\theta}{2} + T(\theta) \sin \frac{d\theta}{2} - dN(\theta) = 0 \quad (1)$$

$$(T(\theta) + dT(\theta)) \cos \frac{d\theta}{2} - T(\theta) \cos \frac{d\theta}{2} - (Q(\theta) + dQ(\theta)) \sin \frac{d\theta}{2} - Q(\theta) \sin \frac{d\theta}{2} - dF(\theta) = 0 \quad (2)$$

$$(M + dM(\theta)) - M(\theta) - (Q(\theta) + dQ(\theta)) \frac{Rd\theta}{2} - Q(\theta) \frac{Rd\theta}{2} - dF(\theta)(R - r) = 0 \quad (3)$$

where $T(\theta)$, $Q(\theta)$, $M(\theta)$, $N(\theta)$, and $F(\theta)$ are the tension, shear, bending moment, normal force, and friction force applied to the gripper, θ is the wrap angle, and R and r are the radius of the gripper and cylindrical bar, respectively. The friction force at the start of sliding is expressed using the coefficient of static friction between the gripper and cylindrical bar, μ , as follows:

$$dF(\theta) = \mu dN(\theta) \quad (4)$$

The following holds if $d\theta$ is infinitesimal:

$$\sin(d\theta/2) \approx d\theta/2 \quad (5)$$

$$\cos(d\theta/2) \approx 1 \quad (6)$$

M can be expressed as follows:

$$M(\theta) = EA\kappa R^2 \left(\frac{1}{R_0} - \frac{1}{R} \right) \quad (7)$$

where E , A , and κ are Young's modulus, cross-sectional area, and section modulus of the gripper, respectively, and R_0 is the radius at the initial state of the gripper. It can be shown that M depends on the radius of curvature; thus, it is constant with respect to the wrap angle θ . Therefore, the following relationship holds:

$$\frac{dM(\theta)}{d\theta} = \frac{d^2M(\theta)}{d\theta^2} = 0 \quad (8)$$

Using the above conditions, the following differential equation is obtained by rearranging the equilibrium equation:

$$\mu(R - r) \frac{d^2T(\theta)}{d\theta^2} + R \frac{dT(\theta)}{d\theta} - \mu r T(\theta) = 0 \quad (9)$$

The solution to this differential equation is as follows:

$$T(\theta) = C_1 \exp(\lambda_1 \theta) + C_2 \exp(\lambda_2 \theta) \quad (10)$$

where λ_1 and λ_2 are as

$$\lambda_1 = \frac{-R + \sqrt{R^2 + 4\mu^2(R - r)r}}{2\mu(R - r)} \quad (11)$$

$$\lambda_2 = \frac{-R - \sqrt{R^2 + 4\mu^2(R - r)r}}{2\mu(R - r)} \quad (12)$$

The boundary conditions is considered. The following is obtained by assuming a constant load spring from 0 deg to 90 deg.

$$T(\pi/2) = F_c \quad (13)$$

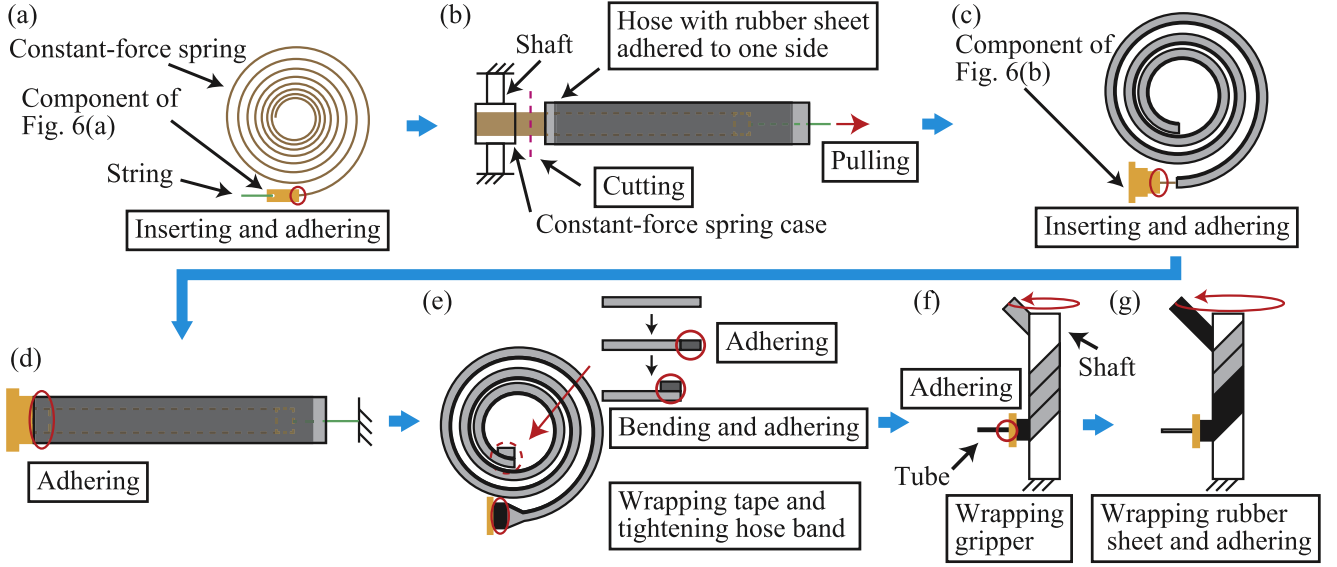


Fig. 5. Fabrication process of the prototype. (a) Insert the component in Fig. 5(a) into constant-force spring. (b) Insert the spring into the hose with the rubber sheet adhered. (c) Insert the component in fig. 5(b) into constant-force spring. (d) Extend hose and adhere base. (e) Close both ends. (f) Wrap gripper around shaft. (g) Wrap a rubber sheet around gripper and adhere.

where F_c denotes the load of the constant-force spring. From (1) and (2), $dT(\theta)/d\theta$ is expressed as follows:

$$\frac{dT(\theta)}{d\theta} = -\frac{r}{R-r}Q(\theta) \quad (14)$$

Therefore, $dT(\theta)/d\theta|_{\theta=\pi/2}$ is expressed as follows:

$$\left. \frac{dT(\theta)}{d\theta} \right|_{\theta=\pi/2} = -\frac{r}{R-r}Q(\pi/2) = 0 \quad (15)$$

From these boundary conditions, C_1 and C_2 can be obtained as follows:

$$C_1 = -\frac{F_c\lambda_2}{\lambda_1 - \lambda_2} \quad (16)$$

$$C_2 = \frac{F_c\lambda_1}{\lambda_1 - \lambda_2} \quad (17)$$

From the above equations, $T(\theta)$ ($\theta > \pi/2$) can be obtained as follows:

$$T(\theta) = -\frac{F_c\lambda_2}{\lambda_1 - \lambda_2} \exp(\lambda_1\theta) + \frac{F_c\lambda_1}{\lambda_1 - \lambda_2} \exp(\lambda_2\theta) \quad (18)$$

In this paper, $T(\theta)$ is defined as the load capacity.

Finally, we consider the variation in $T(\theta)$ with $\theta (\geq \pi/2)$. $\lambda_1 > 0$ and $\lambda_2 < 0$ can be shown by (11), (12), respectively. Hence, $C_1 > 0$ and $C_2 > 0$ by (16), (17). Hence, $T(\theta)$ increases exponentially, and this can be shown by (10). These results indicate that the load capacity of the gripper increases exponentially according to the wrap angle.

IV. PROTOTYPE

Fig. 5 shows the fabrication process of the prototype and describes it in detail.

a) A string is inserted through the hole in the component shown in Fig. 6(a), inserted into and adhered to the tip of

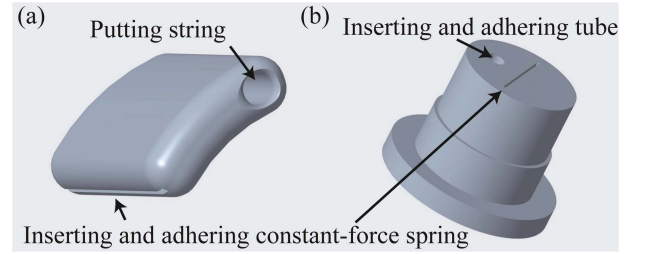


Fig. 6. Components by 3D printing used to fabricate prototype. (a) Insert into tip of constant-force spring. (b) Insert to base of constant-force spring.

- the constant-force spring. This prevents the constant-force spring from breaking through the hose.
- b) Adhere to the rubber sheet with the hose straightened. The rubber sheet prevents abrupt bending of the gripper upon depressurization. A constant-force spring is attached to the rotating shaft and inserted into the hose by pulling the string. During this process, the constant-force spring is inserted to ensure that the rubber sheet is on the side where it is wound. Subsequently, the constant-force spring protruding from the hose is truncated, leaving a few centimeters.
 - c) The protruding constant-force spring is inserted and adhered to the component shown in Fig. 6(b).
 - d) The string is fastened and the constant-force spring is extended to a straightened position. While in this condition, the hose is adhered to the component depicted in Fig. 6(a).
 - e) The open end of the hose is sealed using an adhesive. Subsequently, the section is folded and adhered in place.
 - f) The fabrication is helically wrapped around a cylindrical rod with the same diameter as the inner diameter of the

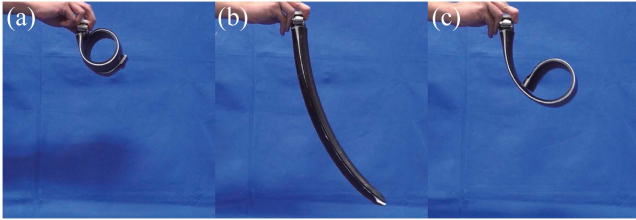


Fig. 7. Vine gripper: (a) Initial state. (b) Pressurize, vine curved due to spring elasticity. (c) No pressurized, vine straighten due to air pressure.

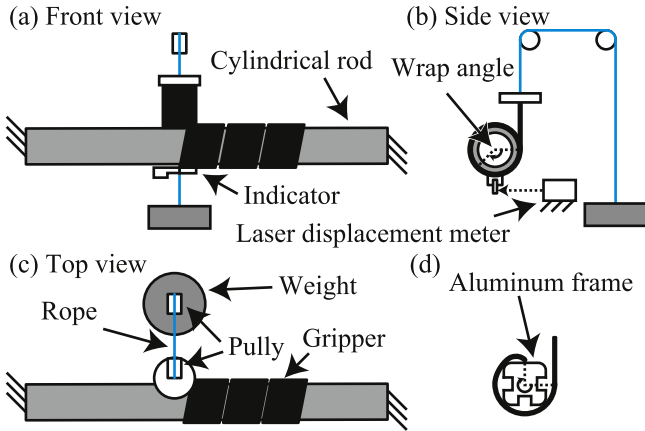


Fig. 8. Schematic diagram of load capacity measurement. (a) Front view. (b) Side view. (c) Top view. (d) Wrapping Aluminum frame.

helical in the fabrication. A tube is inserted and adhered to the component shown in Fig. 6(b).

- g) A rubber sheet is adhered along the fabrication. The rubber sheet functions as a restraining element for the helical wrap angle during depressurization of the gripper.

In this context, a flexible instant adhesive (Henkel AG & Co. KGaA, LPG-010) was utilized to adhere the rubber sheet and the hose, while an instant adhesive (Henkel AG & Co. KGaA, LOCTITE401) was used to adhere to the other components. The weight of the fabricated gripper was 2.5 N and the inner diameter was 60 mm. The load of the constant-force spring was 21.6 N, the rubber sheet was acrylonitrile butadiene rubber, the thickness of the outer rubber sheet was 1 mm, the thickness of the inner rubber sheet was 4 mm, and the hose was a fire hose (IWASAKI MFG, Corp., LTD, 01GLA2520X) of 45 mm width and 25 mm diameter. Fig. 7 shows the gripper pressurized to 0.4 MPa and depressurized to atmospheric pressure. As shown in Fig. 7(a), the gripper is initially wound in a helical shape. When air pressure is applied, it extends to form a straight line as shown in Fig. 7(b), when depressurized to atmospheric pressure, it starts to rewind from the tip as shown in Fig. 7(c), and eventually returns to the initial state.

V. EXPERIMENTS

A. Load Capacity Experiment

The load capacity of this gripper was measured. Fig. 8 shows a schematic diagram of the experiment. Fig. 8(a)–(c) show the

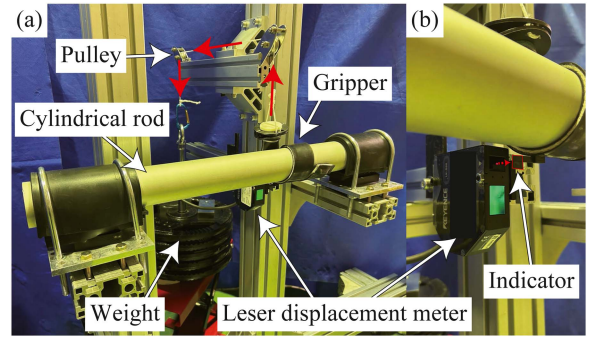


Fig. 9. Setup of load capacity measurement.

front, side, and top view, respectively. The gripper is wrapped around a fixed object that cannot rotate. The base of the gripper is pulled vertically upward, the load is increased and is measured immediately before the gripper slips. In this experiment, the relationship between the wrap angle and load immediately before the gripper slid out was verified. The wrap angle was set as shown in Fig. 8(c). An indicator was attached at wrap angle of 90 deg and the displacement of the indicator was measured using a laser displacement meter (Keyence Co., Ltd., LK-G32) to check whether the gripper was sliding. The displacement of the indicator from before load is applied $d_{\text{indicator}}$ was converted into displacement of the gripper when load is increased d_{gripper} using the following equation.

$$d_{\text{gripper}} = \left(r_{\text{object}} + \frac{t_{\text{gripper}}}{2} \right) \arcsin \left(\frac{d_{\text{indicator}}}{r_{\text{object}} + \frac{t_{\text{gripper}}}{2}} \right) \quad (19)$$

where r_{object} , t_{gripper} are the radius of the object, thickness of the gripper, respectively. Fig. 9 demonstrates the setup of the experiment. The hose and the constant-force spring used for the gripper in this experiment were the same as those used in Section IV. The thickness of the rubber sheet was 1 mm on both sides ($t_{\text{gripper}} = 6$ mm). The gripper was wrapped around an anodized aluminum cylindrical rod with a diameter of 60 mm ($r_{\text{cylindrical rod}} = 60$ mm) and a quadrangular prism (an aluminum frame with 45 mm \times 45 mm and $r_{\text{aluminum frame}} = 64$ mm). The wrap angle of the gripper was increased by 90 deg from 180 deg to 540 deg. The aluminum frame has three grooves as shown in Fig. 9(d), and the aluminum frame is rotated such that the grooves do not come to the tip. First, a weight is hung that does not cause the gripper to slip, and then weights are added. When the object was the cylindrical rod at the wrap angle of 540 deg, the weight was increased by 19.6 N. Otherwise, the weight was increased by 9.8 N. After increasing the weight, displacement of the gripper was measured for 8 min to wait for its displacement fluctuations to decrease and to conform for slippage. It was assumed that the gripper was not sliding when the displacement during the last 1 min was less than 0.01 mm. After each measurement, the inside of the gripper and the surface of the wrapping object were coated with anhydrous ethanol and wiped. This was done to minimize the measurement error. Three measurements were taken for each

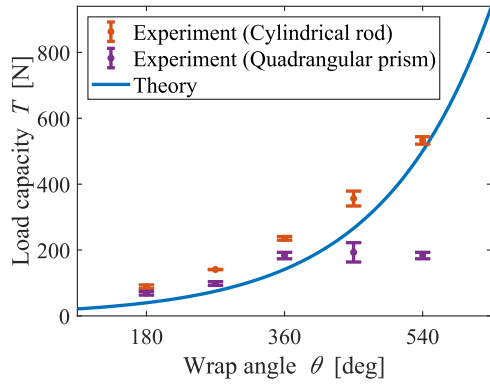


Fig. 10. Result of load capacity measurement.

wrap angle. The measured data were subjected to a fast Fourier transform to remove frequency components above 20 Hz, and were then subjected to an inverse Fourier transform to remove noise. Fig. 10 shows the relationship between the wrap angle and weight immediately prior to sliding out of the gripper. The curve was obtained using Euler's belt theory (18) shown in Section III. In this case, $\mu = 0.4$, $R = 33$ mm and $r = 30$ mm. The result of the cylindrical rod demonstrated that the load capacity increased with the wrap angle, as demonstrated by the extended Euler's belt theory. The result of the quadrangular prism demonstrated the load capacity increases with wrap angle even for objects that are not in perfect contact, unlike the cylindrical rod. The reason why the load capacity is smaller than that of the cylindrical rod is that when the wrap angle increases by 90 deg, the contact area increases by only one corner of the aluminum frame. An increase of one corner does not increase the wrap angle in contact by more than 10 deg. However, the reason why the load capacity does not increase from 450 deg as in that of the cylindrical rod is considered to be that it is difficult to increase the wrap angle in a stable contact state because of the large areas that are not in contact.

B. Adaptability to Object Shapes

The adaptability of the gripper to the shape of the object was verified. In this experiment, the gripper was placed close to an object on the ground with an air pressure of 0.4 MPa applied to it. Subsequently, the gripper was depressurized to atmospheric pressure to confirm whether it could grasp the object. The length of the gripper was 1 m, and the constant-force spring and hose were the same as those used in Section IV. The objects to be grasped were a triangular prism object (140 mm per side, 90 mm high, weight 15.7 N), firewood (weight approximately 4.4 N), a sphere (150 mm diameter, weight 4.12 N), a tripod (weight 14.8 N), a stepladder (weight 20.7 N), a hose (19.2 mm diameter, weight 6.37 N), U-shaped ditch (85 mm high, 110 mm width, 600 mm length, 25 mm thickness, weight 75.0 N), an aluminum frame (30 mm \times 60 mm \times 210 mm, total weight 28.0 N) and torus (approximately 300 mm outer diameter, 250 mm inner diameter, weight 1.27 N). In this experiment, the thicknesses of the rubber sheets on the outside and inside of the gripper were

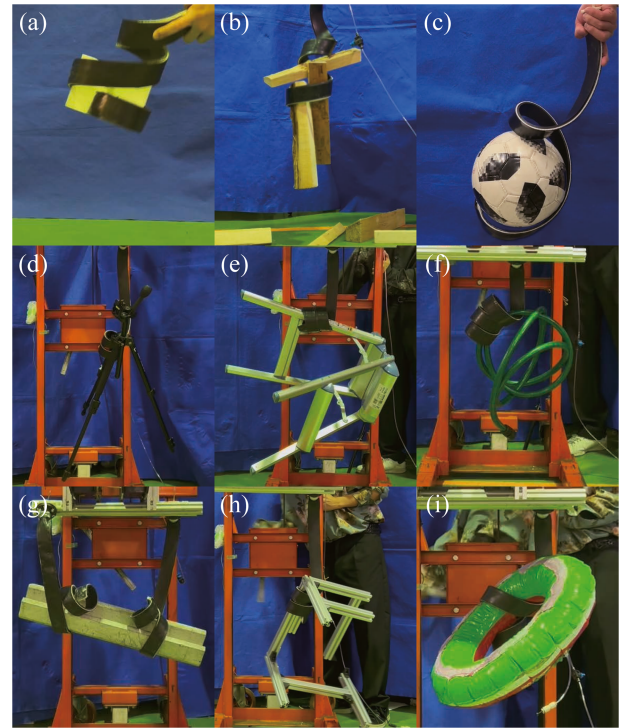


Fig. 11. Adaptability to Object Shapes. (a) Triangular prism. (b) Firewood. (c) Sphere. (d) Tripod. (e) Stepladder. (f) Hose. (g) U-shaped ditch. (h) Aluminum frame. (i) Torus.

1 mm and 4 mm, respectively. The inner diameter of the gripper was 90 mm. Fig. 11 shows how the gripper grasped objects. It was confirmed that the gripper could grasp various shape objects.

C. Twin-Gripper

As described in Section II, a single gripper cannot lift an object that rotates when lifted if its weight exceeds the load of a constant-force spring. However, utilizing a twin-gripper with opposing helical directions enables it to lift objects whose weights exceed the load of a constant-force spring. This is because the direction of the forces that cause each gripper to rotate the object are opposite and cancel each other out. To validate this, an experiment was conducted using a twin-gripper. Fig. 12 illustrates the experiment. Fig. 12(a) illustrates the lifting of the cylindrical bar. A pipe with a diameter of 60 mm was passed through the barbell, and its total weight was 294 N. It was confirmed that the object rotated while being lifted, causing the gripper to unwind and fail to lift. Specifically, a single gripper cannot grasp an object with a load that suppresses the load of the constant-force spring when the object's center of gravity is close to the axis of rotation of the helix drawn by the gripper. Therefore, a twin-gripper was used with the direction of the helix of the grippers reversed, as shown in Fig. 12(b). It was confirmed that the grippers overlap each other as they are wrapped around the gripper. This can be resolved by applying polytetrafluoroethylene (PTFE) adhesive tape to the tip of the gripper. It was confirmed that an object with weight 1660 N, surpassing the load of the constant-force spring, could be grasped, as shown in Fig. 12(c). The gripper was

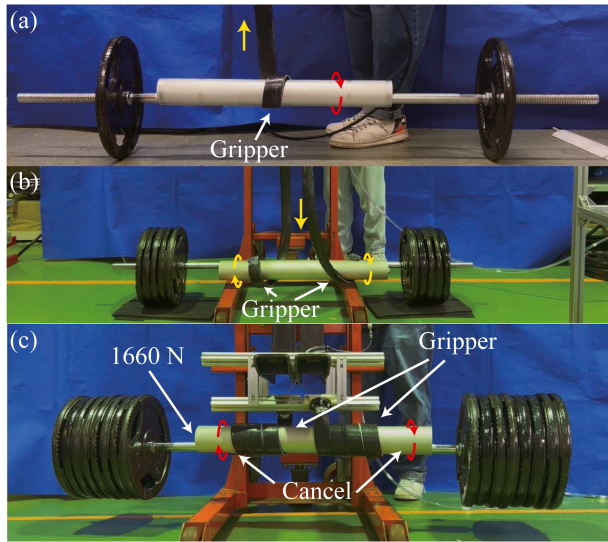


Fig. 12. Grasping by single gripper and twin-gripper (a) Grasping pipe (total weight is 294 N) by single gripper. (b) Twin-gripper wrap around helix in opposite directions. (c) Grasping pipe (total weight is 1660 N) by twin-gripper.

manually wrapped around the cylindrical rod. The cylindrical rod was marked, its displacement was measured by a ruler for 2 min, and the displacement for the last 1 min was less than 0.2 mm, thus it was assumed that the gripper grasped it. The gripper length was 1 m and the thicknesses of the rubber sheets on the outside and inside of the gripper were 0.5 mm and 4 mm, respectively. The reason it can lift an object with a load greater than the constant-force spring is because that the forces exerted by each gripper to rotate the object work in opposite directions, and the rotation is canceled. This experiment demonstrated the capability of grasping a substantial weight despite the small load (43 N) of the constant-force spring.

D. Pick-and-Place Demonstration With Construction Machine Robot

A pick-and-place demonstration was conducted with the grippers attached to a construction machine robot, developed by Yanmar Co., Ltd. Fig. 13 shows the demonstration wherein an object composed of a rebar and concrete (weight 186 N) and a fallen tree model (weight 108 N) were removed. Four grippers are attached to the end of the arm of the construction machine robot as shown in Fig. 13(a). In this experiment, the rubber sheet at the gripper tip was thickened and a warped fitting with PTFE adhesive tape was attached to the gripper tip. Two sets of grippers being pressurized are approaching a fallen tree model as shown in Fig. 13(b). The grippers are lowered with depressurized as shown in Fig. 13(c), and then lowered as shown in Fig. 13(d) and (e). At this moment, the grippers do not slide against a fallen tree model because the force transmitted to the tip is weak. Therefore, the tip slides against a fallen tree model by raising the grippers as in Fig. 13(f). By lowering and raising the gripper as shown in Fig. 13(g) and (h), the gripper wraps around a fallen tree model and can grasp it as shown in Fig. 13(i). The gripper moves the fallen tree as in Fig. 13(j) and releases it as

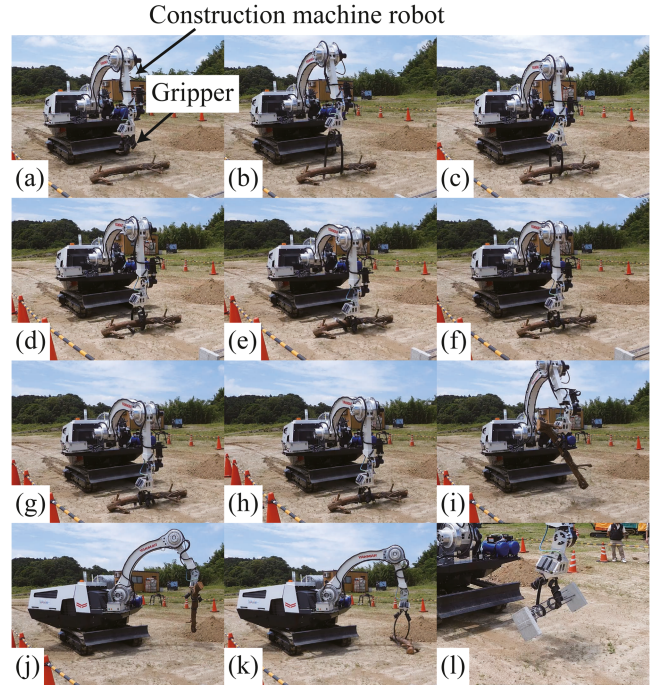


Fig. 13. Demonstration of gripper attached to construction machine robot. (a) Construction machine robot and gripper. (b) Apply air pressure to gripper and approach fallen tree model. (c) Lower gripper with depressurized. (d)(e) Lower gripper. (f) Raise gripper. (g) Lower gripper. (h) Raise gripper. (i) Grasp fallen tree model. (j) Move fallen tree model. (k) Release fallen tree model. (l) Grasp object composed of rebar and concrete.

in Fig. 13(k). Fig. 13(l) shows the gripper grasping a rebar and concrete component.

VI. CONCLUSION

This study presents a vine-like, power soft gripper, which grasps an object by wrapping it. It works stiffly and powerfully only in the tensile direction, resulting in high shape adaptability for objects with various shape. This gripper is based on Euler's belt theory. By extending the belt as a curved beam, it is shown that this gripper increases exponentially according to the wrap angle. Therefore, a prototype was fabricated to verify the load capacity and shape adaptability of the gripper. The load capacity measurement experiment demonstrated that the load capacity increased with the wrap angle, as indicated by the extended belt theory. The grasping experiment to verify the shape adaptability confirmed that the gripper could grasp various shape objects. Furthermore, it was confirmed that the twin-gripper each with opposite helical directions could grasp an object that rotated when lifted, whereas one gripper could not grasp an object that exceeded the load of the constant-force spring. The load of the two constant-force springs used was 43 N, which was small. However, it was demonstrated that an object weighing 1660 N could be grasped. Furthermore, the load capacity is even higher for some applications because the gripper is assumed to be sliding when its displacement is 0.01 mm or greater. Finally, the gripper was attached to the construction machine robot and a pick-and-place demonstration was conducted. With regard

to these factors, it is considered possible to grasp and move irregularly shaped heavy objects at sites where they are handled, such as disaster sites based on a combination with a construction machine robot.

These results indicate that the proposed gripper is a soft gripper that combines the high load capacity and shape adaptability. In addition to improving the performance of the gripper, further field tests will be conducted to verify the gripper's load capacity, shape adaptability, and behavior when the gripper is damaged.

ACKNOWLEDGMENT

The authors would like to thank Yanmar Company Ltd. for their cooperation in conducting the pick-and-place demonstration.

REFERENCES

- [1] J. Shintake, V. Cacucciolo, D. Floreano, and H. Shea, "Soft robotic grippers," *Adv. Mater.*, vol. 30, no. 29, 2018, Art. no. 1707035, doi: [10.1002/adma.201707035](https://doi.org/10.1002/adma.201707035).
- [2] L. Zhou, L. Ren, Y. Chen, S. Niu, Z. Han, and L. Ren, "Bio-inspired soft grippers based on impactive gripping," *Adv. Sci.*, vol. 8, no. 9, 2021, Art. no. 2002017, doi: [10.1002/advs.202002017](https://doi.org/10.1002/advs.202002017).
- [3] A. K. Mishra, E. Del Dottore, A. Sadeghi, A. Mondini, and B. Mazzolai, "SIMBA: Tendon-driven modular continuum arm with soft reconfigurable gripper," *Front. Robot. AI*, vol. 4, 2017, doi: [10.3389/frobot.2017.00004](https://doi.org/10.3389/frobot.2017.00004).
- [4] M. Manti, T. Hassan, G. Passetti, N. D'Elia, C. Laschi, and M. Cianchetti, "A bioinspired soft robotic gripper for adaptable and effective grasping," *Soft Robot.*, vol. 2, no. 3, pp. 107–116, 2015, doi: [10.1089/soro.2015.0009](https://doi.org/10.1089/soro.2015.0009).
- [5] M. Tavakoli et al., "Autonomous selection of closing posture of a robotic hand through embodied soft matter capacitive sensors," *IEEE Sensors J.*, vol. 17, no. 17, pp. 5669–5677, Sep. 2017.
- [6] K. Suzumori, S. Iikura, and H. Tanaka, "Development of flexible microactuator and its applications to robotic mechanisms," in *Proc. IEEE Int. Conf. Robot. Automat.*, 1991, pp. 1622–1623, doi: [10.1109/ROBOT.1991.131850](https://doi.org/10.1109/ROBOT.1991.131850).
- [7] B. S. Homberg, R. K. Katzschmann, M. R. Dogar, and D. Rus, "Haptic identification of objects using a modular soft robotic gripper," in *Proc. IEEE/RSJ Int. Conf. Intell. Robots Syst.*, 2015, pp. 1698–1705.
- [8] F. Ilievski, A. D. Mazzeo, R. F. Shepherd, X. Chen, and G. M. Whitesides, "Soft robotics for chemists," *Angewandte Chemie Int. Ed.*, vol. 50, no. 8, pp. 1890–1895, 2011, doi: [10.1002/anie.201006464](https://doi.org/10.1002/anie.201006464).
- [9] H. Zhang, A. S. Kumar, F. Chen, J. Y. H. Fuh, and M. Y. Wang, "Topology optimized multimaterial soft fingers for applications on grippers, rehabilitation, and artificial hands," *IEEE/ASME Trans. Mechatronics*, vol. 24, no. 1, pp. 120–131, Feb. 2019.
- [10] W. Wang, C. Li, M. Cho, and S.-H. Ahn, "Soft tendril-inspired grippers: Shape morphing of programmable polymer–paper bilayer composites," *ACS Appl. Mater. Interfaces*, vol. 10, no. 12, pp. 10419–10427, Mar. 2018, doi: [10.1021/acsami.7b18079](https://doi.org/10.1021/acsami.7b18079).
- [11] M. Yang, L. P. Cooper, N. Liu, X. Wang, and M. P. Fok, "Twining plant inspired pneumatic soft robotic spiral gripper with a fiber optic twisting sensor," *Opt. Exp.*, vol. 28, no. 23, pp. 35158–35167, Nov. 2020. [Online]. Available: <https://opg.optica.org/oe/abstract.cfm?URI=oe-28-23-35158>
- [12] J. R. Amend, E. Brown, N. Rodenberg, H. M. Jaeger, and H. Lipson, "A positive pressure universal gripper based on the jamming of granular material," *IEEE Trans. Robot.*, vol. 28, no. 2, pp. 341–350, Apr. 2012.
- [13] Y. Wang et al., "Inflatable particle-jammed robotic gripper based on integration of positive pressure and partial filling," *Soft Robot.*, vol. 9, no. 2, pp. 309–323, 2022, doi: [10.1089/soro.2020.0139](https://doi.org/10.1089/soro.2020.0139).
- [14] Z. Xie et al., "Octopus arm-inspired tapered soft actuators with suckers for improved grasping," *Soft Robot.*, vol. 7, no. 5, pp. 639–648, 2020, doi: [10.1089/soro.2019.0082](https://doi.org/10.1089/soro.2019.0082).
- [15] M. Wu et al., "Glowing sucker octopus (*Stauroteuthis syrtensis*)-inspired soft robotic gripper for underwater self-adaptive grasping and sensing," *Adv. Sci.*, vol. 9, no. 17, 2022, Art. no. 2104382, doi: [10.1002/advs.202104382](https://doi.org/10.1002/advs.202104382).
- [16] B. Mazzolai et al., "Octopus-inspired soft arm with suction cups for enhanced grasping tasks in confined environments," *Adv. Intell. Syst.*, vol. 1, no. 6, 2019, Art. no. 1900041, doi: [10.1002/aisy.201900041](https://doi.org/10.1002/aisy.201900041).
- [17] H. Tian et al., "Gecko-effect inspired soft gripper with high and switchable adhesion for rough surfaces," *Adv. Mater. Interfaces*, vol. 6, no. 18, 2019, Art. no. 1900875, doi: [10.1002/admi.201900875](https://doi.org/10.1002/admi.201900875).
- [18] V. Alizadehyazdi, M. Bonthron, and M. Spenko, "An electrostatic/gecko-inspired adhesives soft robotic gripper," *IEEE Robot. Automat. Lett.*, vol. 5, no. 3, pp. 4679–4686, Jul. 2020.
- [19] P. Glick, S. A. Suresh, D. Ruffatto, M. Cutkosky, M. T. Tolley, and A. Parness, "A soft robotic gripper with gecko-inspired adhesive," *IEEE Robot. Automat. Lett.*, vol. 3, no. 2, pp. 903–910, Apr. 2018.
- [20] H. Li, J. Yao, P. Zhou, W. Zhao, Y. Xu, and Y. Zhao, "Design and modeling of a high-load soft robotic gripper inspired by biological winding*," *Bioinspiration Biomimetics*, vol. 15, no. 2, Feb. 2020, Art. no. 026006, doi: [10.1088/1748-3190/ab6033](https://doi.org/10.1088/1748-3190/ab6033).
- [21] T. Hu, X. Lu, and D. Xu, "A dual-mode and enclosing soft robotic gripper with stiffness-tunable and high-load capacity," *Sensors Actuators A: Phys.*, vol. 354, 2023, Art. no. 114294. [Online]. Available: <https://www.sciencedirect.com/science/article/pii/S0924424723001437>
- [22] D. Sui, T. Wang, S. Zhao, X. Zhang, J. Zhao, and Y. Zhu, "An enveloping soft gripper with high-load carrying capacity: Design, characterization and application," *IEEE Robot. Automat. Lett.*, vol. 7, no. 1, pp. 373–380, Jan. 2022.
- [23] H. Li, P. Zhou, S. Zhang, J. Yao, and Y. Zhao, "A high-load bioinspired soft gripper with force booster fingers," *Mechanism Mach. Theory*, vol. 177, 2022, Art. no. 105048. [Online]. Available: <https://www.sciencedirect.com/science/article/pii/S0094114X22002956>
- [24] J. T. Kim et al., "Development of disaster-responding special-purpose machinery: Results of experiments," *J. Field Robot.*, vol. 39, no. 6, pp. 783–804, 2022, doi: [10.1002/rob.22078](https://doi.org/10.1002/rob.22078).
- [25] T. Nishida, H. Koga, Y. Fuchikawa, Y. Kitayama, S. Kurogi, and Y. Arimura, "Development of pilot assistance system with stereo vision for robot manipulation," in *Proc. SICE-ICASE Int. Joint Conf.*, 2006, pp. 2675–2680.
- [26] R. V. Martinez et al., "Robotic tentacles with three-dimensional mobility based on flexible elastomers," *Adv. Mater.*, vol. 25, no. 2, pp. 205–212, 2013, doi: [10.1002/adma.201203002](https://doi.org/10.1002/adma.201203002).
- [27] H. Amase, Y. Nishioka, and T. Yasuda, "Mechanism and basic characteristics of a helical inflatable gripper," in *Proc. IEEE Int. Conf. Mechatronics Automat.*, 2015, pp. 2559–2564.
- [28] T. T. Hoang, P. T. Phan, M. T. Thai, N. H. Lovell, and T. N. Do, "Bio-inspired conformable and helical soft fabric gripper with variable stiffness and touch sensing," *Adv. Mater. Technol.*, vol. 5, no. 12, 2020, Art. no. 2000724, doi: [10.1002/admt.202000724](https://doi.org/10.1002/admt.202000724).